Quantitative Optical Spectroscopy: A Robust Tool for Direct Measurement of Breast Cancer Vascular Oxygenation and Total Hemoglobin Content *In vivo*

J. Quincy Brown,[1] Lee G. Wilke,[2] Joseph Geradts,[3] Stephanie A. Kennedy,[1] Gregory M. Palmer,[4] and Nirmala Ramanujam[1]

[1]Department of Biomedical Engineering, Duke University; Departments of [2]Surgery, [3]Pathology, and [4]Radiation Oncology, Duke University Medical Center, Durham, North Carolina

Abstract

We propose the use of a robust, biopsy needle–based, fiber-optic tool for routine clinical quantification of tumor oxygenation at the time of diagnostic biopsy for breast cancer. The purpose of this study was to show diffuse reflectance spectroscopy as a quantitative tool to measure oxygenation levels in the vascular compartment of breast cancers *in vivo* via an optical biopsy technique. Thirty-five patients undergoing surgical treatment for breast cancer were recruited for the study at Duke University Medical Center. Diffuse reflectance spectroscopy was performed on the tumors *in situ* before surgical resection, followed by needle-core biopsy of the optically measured tissue. Hemoglobin saturation and total hemoglobin content were quantified from 76 optical spectra-tissue biopsy pairs, consisting of 20 malignant, 23 benign, and 33 adipose tissues. Hemoglobin saturation in malignant tissues was significantly lower than nonmalignant tissues ($P < 0.002$) and was negatively correlated with tumor size and pathologic tumor category ($P < 0.05$). Hemoglobin saturation was positively correlated with total hemoglobin content in malignant tissues ($P < 0.02$). HER2/neu-amplified tumors exhibited significantly higher total hemoglobin content ($P < 0.05$) and significantly higher hemoglobin saturation ($P < 0.02$), which is consistent with a model of increased angiogenesis and tumor perfusion promoted by HER2/neu amplification. Diffuse reflectance spectroscopy could aid in prognosis and prediction in breast cancer via quantitative assessment of tumor physiology at the time of diagnostic biopsy. [Cancer Res 2009;69(7):2919–26]

Introduction

Tumor growth is facilitated by hypoxia or low oxygen tension in tissue (1). Direct measurement of tumor hypoxia has been linked to decreased overall survival and increased risk of local recurrence in several organ sites, including the uterine cervix (2), head and neck cancers (3), and soft tissue sarcomas (4). Overexpression of biomarkers related to hypoxia [hypoxia-inducible factor-1α (HIF-1α) and carbonic anhydrase 9 protein (CA IX)] in breast cancer has also been linked to poor prognosis (5). Hypoxia has been implicated in the resistance of tumors to radiation and some types of chemotherapy (6, 7) and is a predictor of response (8, 9). The aggressiveness of hypoxic tumors is likely related to the selective adaptation of hypoxia-resistant tumor phenotypes, which can thrive in low-oxygen environments. Numerous studies have investigated the link between clinical outcomes and hypoxia using a variety of different methods to date (8). All of these studies have shown that hypoxia is clearly related to clinical outcome, which motivates the importance of measuring hypoxia in the clinical setting.

Based on the number of studies that relate various measures of hypoxia with clinical outcomes in the breast, it is clear that routine measurement of pretreatment tumor oxygenation in the breast would be attractive to physicians due to its potential prognostic and predictive value. However, the combined disadvantages of currently available methods have translated to the lack of routine clinical measurements of breast tumor hypoxia. We propose the use of a simple-to-use, robust, fiber-optic probe, which is compatible with biopsy needles commonly used in routine diagnostic biopsy of the breast, to provide an immediate and nondestructive measurement of tumor vascular oxygenation *in vivo* using a technique called diffuse reflectance spectroscopy. This optical method is label-free, does not require an oxygen standard for calibration, has a signal-to-noise ratio that is independent of oxygenation, does not consume oxygen, and is not susceptible to electromagnetic interference. Diffuse reflectance spectroscopy provides a measurement of the absorption, and scattering, of the tissue from cubic millimeter (UV-visible wavelengths) to cubic centimeter volumes (near-IR wavelengths). The absorption and scattering, or optical properties, of the tissues are reflective of their physiologic and structural composition. The primary absorbers in breast tissue include oxygenated (HbO_2) and deoxygenated (Hb) hemoglobin (absorption in the UV-visible and near-IR wavelengths), β-carotene (visible wavelengths), as well as lipids and water (near-IR wavelengths).

Our group has developed a novel optical toolbox to perform quantitative physiology *in vivo*, which has been extensively tested in a laboratory setting (10, 11) and in preclinical models (12, 13). This toolbox consists of an optical spectrometer coupled to custom-designed fiber-optic probes for delivery and collection of light from tissue, which are compatible with commonly used biopsy or endoscopy devices. In addition, the toolbox includes a series of stochastic Monte Carlo models, which extract tissue absorption and scattering from diffuse reflectance measurements (11) as well as the contribution of intrinsic tissue fluorophores (14) from the tissue fluorescence spectra. The objective of the current study was to show the capability and utility of this toolbox to directly measure breast tumor oxygenation *in vivo*. Ultrasound guidance was used to interface the fiber-optic probe with normal and cancerous tissues in patients undergoing surgical treatment

Requests for reprints: J. Quincy Brown, Department of Biomedical Engineering, Duke University, 136 Hudson Hall, Box 90281, Durham, NC 27708. Phone: 919-660-8465; Fax: 919-684-4488; E-mail: quincy.brown@duke.edu.

©2009 American Association for Cancer Research.

doi:10.1158/0008-5472.CAN-08-3370

Downloaded from http://aacrjournals.org/cancerres/article-pdf/69/7/2919/2622523/2919.pdf by guest on 14 September 2024

for stage I to stage IIIA breast cancer before surgical resection, ensuring that measurements came from tissues in their vascularized and nascent state. The measurements were made on patients undergoing surgery rather than on those undergoing core needle biopsy to increase the tumor measurement yield. The focus of this report is to present our quantitative measurements of tumor physiology via diffuse reflectance spectroscopy and to show its potential utility as a prognostic/predictive tool.

Materials and Methods

Instrumentation. Custom-designed fiber-optic probes were manufactured by Polymicro Technologies, Inc. and RoMack, Inc. with surgical stainless steel jacketing. Two probe tip designs were used: probe A had an outer diameter of 3.47 mm, whereas probe B had an outer diameter of 2.1 mm. The lengths and diameters of probes A and B were designed to fit into the lumens of 10-gauge and 14-gauge biopsy cannulas, respectively. Each probe shared a common illumination and collection fiber arrangement, namely, a bundle of nineteen 200-μm illumination fibers arranged to have an effective illumination area with a diameter of 1 mm, surrounded by a concentric ring (probe A, 4; probe B, 18) of 200-μm collection fibers. Probes A and B have been described in our previous publications (15, 10). Although probe A has 16 fewer collection fibers than probe B, in both probes, the collection fibers are close packed and evenly spaced around the 19-fiber illumination core. Thus, the average fiber-to-fiber spacing between the two probes is not significantly different, ensuring that the sensing depth of each probe was approximately the same (simulated to be 0.6–2 mm, depending on wavelength-dependent optical properties). However, because probe A had fewer collection fibers, the collected signal was lower than probe B, requiring longer CCD integration times, in general, during data collection. The probes were designed such that, when fully inserted, they extended past the end of the biopsy cannula only far enough to fill the cavity left by the needle used to introduce the cannula. This was to minimize, as much as possible, any artifact due to variations in pressure, although there currently is no mechanism to provide feedback to the user as to how much pressure is being applied. The fiber-optic probes were coupled to an optical spectrometer. The optical spectrometer used in this study consisted of a 450 W xenon arc lamp, double excitation monochromator (Gemini 180), imaging spectrograph (TRIAX 320), and Peltier-cooled CCD (Symphony) from Jobin-Yvon HORIBA. The fiber probes were sterilized with low-temperature ethylene oxide gas before use in the patient studies.

Clinical study design. This study was approved by the Institutional Review Board at Duke University in accordance with assurances filed with and approved by the Department of Health and Human Services. Informed consent for study participation was obtained from 35 eligible participants. Patients undergoing either a modified radical mastectomy or partial mastectomy for invasive and noninvasive breast malignancies, with lesions of at least 1 cm in diameter, were recruited for study participation. Demographic and pathologic data were collected for each patient who offered informed consent.

Optical spectroscopy of the breast *in vivo* was performed in the operating room before resection of the tumor or removal of the breast. Patients in this study underwent local anesthesia via thoracic paravertebral block, which is the standard of care at our institution. The sterilized optical probes were handled by a surgeon (L.G.W.) under a sterile field, whereas the other end that couples to the instrument was handed to the spectrometer operators for connection to the light source and detector. The operating room lights were turned off during optical spectroscopy, and the theater lights were directed away from the operating field during each measurement to prevent contamination from ambient light. The surgeon located the lesion under ultrasound guidance; then, either a 10-gauge or 14-gauge biopsy needle coaxial cannula (Bard "Vacora" or Cardinal Health "Achieve") was guided through a small incision in the skin into the region of interest. After the cannula was in the region of interest, the needle was removed (leaving the cannula in place), and the cannula was flushed with sterile saline to remove any residual blood in the field. Then, the appropriate fiber-optic probe (10-gauge or 14-gauge diameter) was inserted through the cannula and interfaced with the tissue at a distance of 2 mm past the cannula. A diffuse reflectance measurement (350–600 nm) was collected, the optical probe was retracted, and a biopsy needle (10-gauge Bard Vacora, 14-gauge Bard Vacora, or 14-gauge Cardinal Achieve) was inserted through the cannula and a biopsy sample was removed. This resulted in the removal of a typically 20-mm-long cylinder of tissue, the proximal end of which corresponded to the volume optically measured by the probe. Coregistration of the biopsied tissue with the optically measured area was independently verified in a separate experiment on reduction mammoplasty tissue. Both biopsy devices maintained the orientation of the tissue on removal of the tissue from the biopsy device. The end of the biopsy core distal to the optical probe was marked with India ink to preserve orientation and immediately placed in 10% buffered formalin. The above procedure was typically repeated at one to two more sites for each patient (two to three sites total). The entire process took on average 10 min of operating time. Immediately after collection of tissue spectra, reflectance calibration measurements were performed by inserting the tip of the probe into an integrating sphere (Labsphere). Tissue reflectance spectra were calibrated for the wavelength-dependent throughput of the system by dividing the tissue spectra point by point by the integrating sphere diffuse reflectance spectrum for each patient study.

Tissue processing, pathologic review, and tissue classification. Biopsy samples were processed via standard histologic procedures. After paraffin embedding, the cores were sectioned along the long axis of the biopsy cores. Tissue sections were obtained longitudinally at three levels (denoted as top, middle, and bottom of the core) and stained with H&E. The resulting tissue sections were scored by a board-certified pathologist (J.G.), with special attention being paid to the proximal 3 mm of the core corresponding to the optical measurement, opposite the end marked with India ink. Both the proximal ends and whole cores were given an overall classification as normal, benign, or malignant. The proximal end of the core only was also scored for tissue composition—percentage of epithelium, stroma, fat, and hemorrhage for normal/benign tissues and percentage of benign epithelium, stroma, fat, *in situ* carcinoma, invasive carcinoma, and hemorrhage for malignant tissues. Table 1 contains a detailed histologic breakdown of the tissue samples used in the study.

Pathologically confirmed final tumor size, tumor category, nodal status, and Nottingham combined tumor grade were determined from the surgical pathology report. Menopausal status and chemotherapy status (neoadjuvant chemotherapy versus no prior chemotherapy) were obtained from the patients' medical records. Estrogen receptor (ER), progesterone receptor (PR), and epidermal growth factor receptor (EGFR) status were determined via immunohistochemistry. HER2/neu receptor status of tumor tissues was determined via a combination of immunohistochemistry and fluorescence

Table 1. Histologic breakdown of tissue samples used for data analysis

Type	Subtype	*n*	Subtotal
Malignant	Invasive ductal carcinoma	15	
	Invasive lobular carcinoma	1	
	Mixed invasive ductal-lobular carcinoma	2	
	Ductal carcinoma *in situ*	2	20
Benign	Normal breast (<50% adipose)	11	
	Fibrocystic change	2	
	Fibrosis	5	
	Mixed fibrosis-fibrocystic change	1	
	Fat necrosis	2	
	Biopsy site	1	
	Muscle	1	23
Adipose	Normal breast (>50% adipose)		33
Total			76

Downloaded from http://aacrjournals.org/cancerres/article-pdf/69/7/2919/2622523/2919.pdf by guest on 14 September 2024

in situ hybridization (FISH). To dichotomize the results as positive and negative for HER2, immunohistochemistry membrane expression scores (Dako HercepTest) of 0+ and 1+ were classified as HER2 negative, and scores of 3+ were classified as HER2 positive. For tissues with an immunohistochemical score of 2+, the results of *HER2* gene amplification by FISH were used to classify these tissues as HER2 negative (HER2 gene not amplified) or HER2 positive (*HER2* gene amplified).

Extraction of tissue optical properties. An inverse Monte Carlo model previously developed by our group was used to extract scattering and absorption properties of the measured tissues. Details about this model are available elsewhere (11, 16). Diffuse reflectance spectra measured from tissue were fit over the wavelength range of 400 to 600 nm. The free parameters related to absorption were the concentrations of the intrinsic absorbers assumed to be present in this wavelength range (i.e., Hb, HbO_2, and β-carotene). Lymphazurin (Tyco Healthcare), a blue dye used to locate the sentinel node during surgery, was also included as an extrinsic absorber because it was present in some of the samples. The fixed absorption parameters were the extinction coefficients of oxygenated and deoxygenated hemoglobin and β-carotene, which were obtained from an online database, whereas the absorption spectrum of Lymphazurin was measured separately in our laboratory. A Gaussian-shaped absorber with a center wavelength of 515 nm and a full-width half-maximum of 10 nm was used as well to account for deviations in the model fits thought to be due to differences in the absorption of β-carotene *in vivo* (15). For scattering, the fixed parameters were the refractive indices of the scatterers and the surrounding medium, and the anisotropy factor, whereas the free parameters were the size and density of the spherical scatterers. All fits and subsequent data analysis were performed using MATLAB 7.1 (The MathWorks).

Statistical analysis. For data analysis, the percentage of tissue types for each tissue sample was averaged over the three section levels to give the average percentage of tissue type for each core, assumed to be representative of the entire proximal 3 mm of the biopsy core. For comparison purposes, the tissue samples were grouped into several classes. Tissue samples were reclassified from the proximal tissue type percentages as adipose (>50% fat content, without malignant pathology), benign (normal or benign pathology with <50% fat), or malignant (any *in situ* or invasive carcinoma present). Tissue samples were further classified as simply nonmalignant or malignant based on this reclassification. Nonmalignant samples were grouped by menopausal status, whereas malignant samples were grouped by receptor status, menopausal status, and chemotherapy status for more detailed statistical analysis. Unpaired Student's t tests and Wilcoxon rank-sum tests were used (on the means and medians, respectively) to determine whether statistically significant differences between tissue types, subgroups, and diagnoses existed in parameters extracted from the diffuse reflectance spectra. Correlations were evaluated by computing Spearman's ρ (rank correlation). All statistical analyses were performed using the Statistics Toolbox in MATLAB.

Results

Representative diffuse reflectance spectra (calibrated for system throughput) are shown in Fig. 1 for benign and malignant tissues. As expected, the benign tissue spectrum (Fig. 1*A*) is dominated by oxyhemoglobin absorption as evidenced by the prominent α and β absorption bands between 550 and 580 nm. Figure 1*B* and *C*, however, shows the variability in oxygenation status for malignant tissues, with the malignant spectrum in Fig. 1*C* being dominated by deoxyhemoglobin (as evidenced by the lack of distinct α and β absorption bands and the slight red shift of the Soret band at ~420 nm) in contrast to the more oxygenated malignant tissue of Fig. 1*B*. Extracted sO_2 values, quantified using the inverse model (11, 16), for each of these tissues are given in the figures as well. The malignant sample of Fig. 1*B* was positive for the HER2/neu receptor, whereas the malignant tissue of Fig. 1*C* was negative for

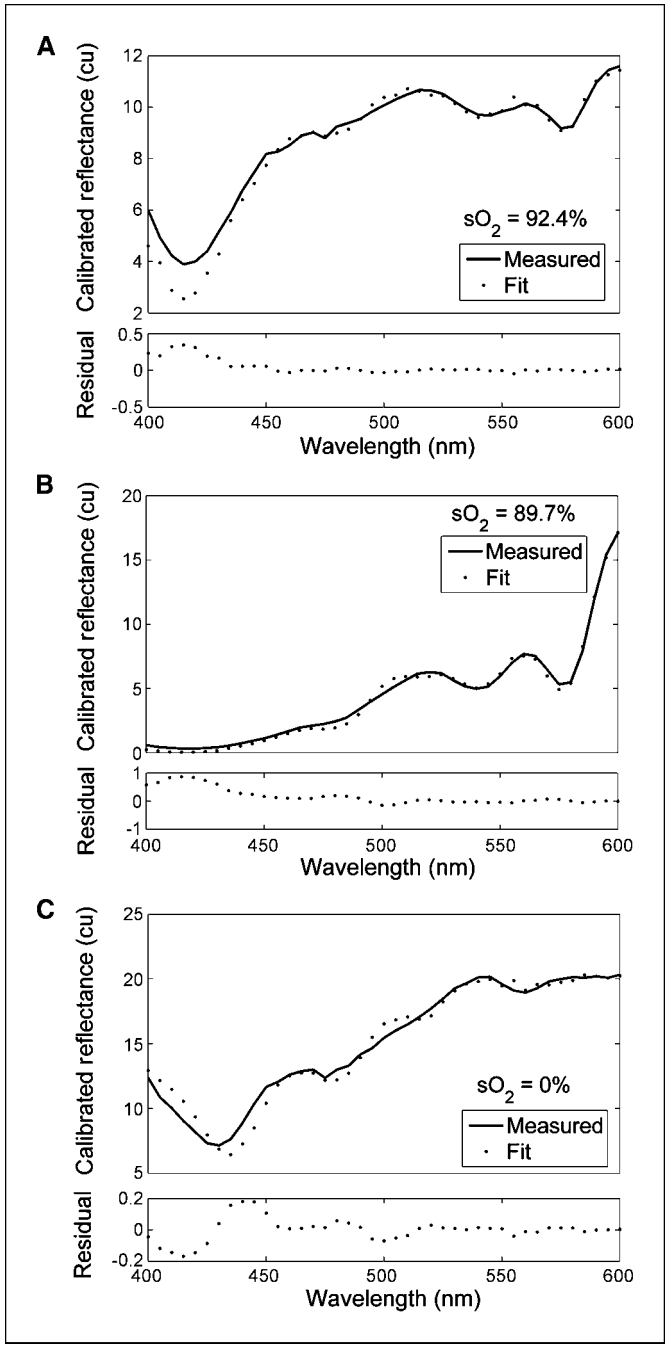

Figure 1. Representative calibrated diffuse reflectance spectra and model fits for benign (*A*), $HER2^+$ malignant (*B*), and $HER2^-$ malignant (*C*) tissues. Corresponding extracted hemoglobin saturation (sO_2) values are indicated above the figure legends.

HER2. Table 2 gives THb and sO_2 values of breast tissue vasculature *in vivo*, stratified by tissue type. The mean and median values of sO_2 for malignant tissues were significantly lower than benign, adipose, and all nonmalignant tissue types. Both the mean and median sO_2 values were ~50% of the values for the nonmalignant categories. The sO_2 values of benign and adipose tissues were not statistically different. Neither the mean nor the median value of THb for malignant tissues was statistically different from those of benign, adipose, or all nonmalignant tissues. However, the mean value of THb for malignant tissues was ~4 μmol/L higher than

Downloaded from http://aacrjournals.org/cancerres/article-pdf/69/7/2919/2622523/2919.pdf by guest on 14 September 2024

Table 2. Results of hemoglobin saturation (sO_2) and total hemoglobin content (THb) measurements for all tissues, stratified by tissue type

	n	Hemoglobin saturation (%)				Total hemoglobin (μmol/L)			
		Mean	*P*	Median	*P*	Mean	*P*	Median	*P*
Malignant	20	44.5		38.9		17		10.3	
All nonmalignant	56	81.9	<5e−7	86.5	<0.0001	13.5	n.s.	9.3	n.s.
Benign	23	83.7	<0.0001	84.9	<0.005	13.6	n.s.	8.5	n.s.
Adipose	33	80.6	<0.0001	87.4	<0.005	13.4	n.s.	10.2	n.s.

NOTE: The *P* values for the mean (unpaired Student's *t* test) and median (Wilcoxon rank-sum) are given to indicate which tissue types were significantly different from malignant.

those of benign, adipose, and all nonmalignant tissues, which only varied by 0.2 μmol/L between the three categories. Whereas there seems to be a (nonsignificant) trend in a higher mean THb in malignant tissues, that same trend was not observed in the median THb values.

Figure 2 contains sO_2 histograms given in relative frequency for (*A*) malignant, (*B*) all nonmalignant, (*C*) benign, and (*D*) adipose tissues. These histograms are useful in graphically representing the distribution of sO_2 for tissues in both nonmalignant and malignant categories. Thirty percent of malignant tissues exhibit sO_2 values between 0% and 2.5%, and the majority (60%) of malignant tissues exhibit sO_2 values <75%. For malignant samples with sO_2 values >75%, most (75%) were from stage I and stage IIA lesions, whereas the remaining 25% were equally split between stage IIB and stage IIIA lesions. None of the samples from stage I lesions had sO_2 values <75%. Sixty percent of stage II+ cancers had sO_2 values <75%. Although the trend was for decreased sO_2 with increased cancer stage, no significant correlation between sO_2 and cancer stage could be established.

Nonmalignant tissues (Fig. 2*B–D*) show a probability distribution weighted toward higher sO_2 values. Thirty-four percent of nonmalignant tissues exhibited saturation values between 95% and 100% of sO_2. The majority (73%) of nonmalignant tissue samples exhibited hemoglobin saturations >75%. Benign tissues (Fig. 2*C*) seemed to exhibit less variability in sO_2 than adipose tissues (Fig. 2*D*); although the overall range of sO_2 values was similar between the two categories, unlike benign tissues, adipose tissues were distinct in that a small percentage (6%) exhibit sO_2 values <40%.

Although there was no significant correlation between sO_2 and cancer stage (which incorporates tumor size, axillary lymph node

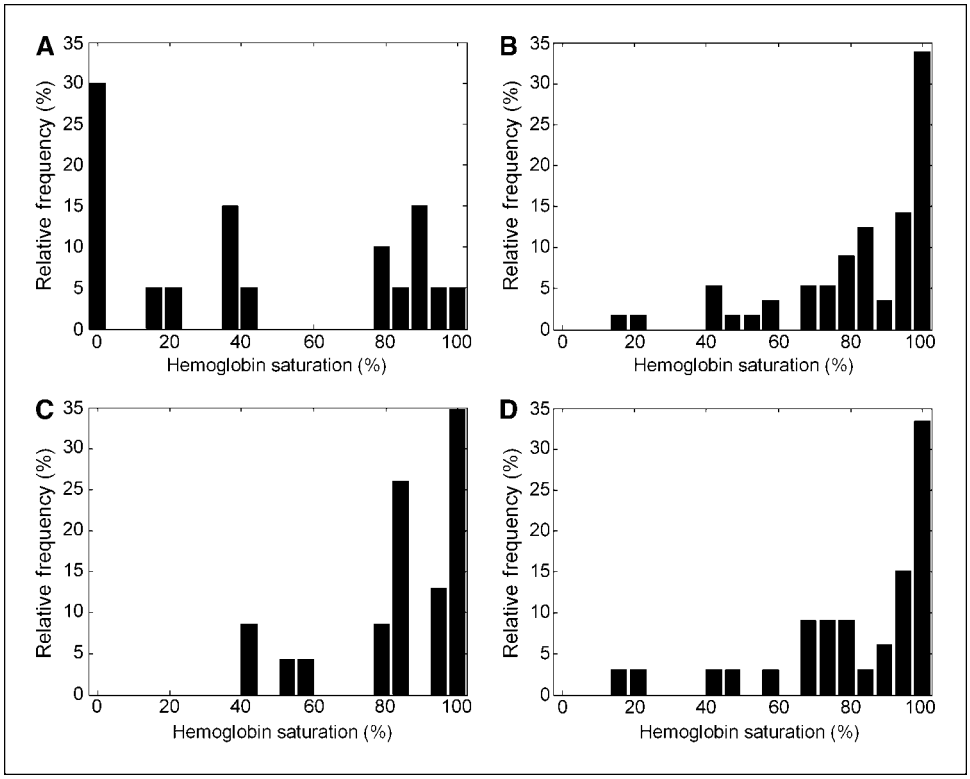

Figure 2. Tissue hemoglobin saturation histograms for malignant (*A*), nonmalignant (*B*), benign (*C*), and adipose (*D*) tissues.

Downloaded from http://aacrjournals.org/cancerres/article-pdf/69/7/2919/2622523/2919.pdf by guest on 14 September 2024

status, and distant metastases), there was a correlation between sO_2 and tumor size alone. Figure 3*A* shows a plot of tissue hemoglobin saturation versus tumor size for all malignant tissues. sO_2 of tumor tissue was negatively correlated with overall invasive tumor size ($\rho = -0.50$, $P < 0.05$), as well as pathologic tumor category ($\rho = -0.49$, $P < 0.05$). The observed relationship between sO_2 and tumor size is consistent with a study in an ectopic rodent model, which noted the same relationship (17). sO_2 was not correlated with the percentage of malignancy in the biopsied tissue ($\rho = 0.12$, $P = 0.62$), nor was it correlated with lymph node status or Nottingham histologic grade. Figure 3*B* presents sO_2 as a function of THb content in malignant tissues only. sO_2 was positively correlated with THb ($P < 0.02$) in malignant tissues, but not in nonmalignant tissues ($P = 0.60$; data not shown).

Malignant and nonmalignant tissues were further divided into subgroups based on menopausal status, chemotherapy status, and tumor receptor status (malignant tissues only). No significant differences were observed in nonmalignant tissues based on menopausal status or chemotherapy status. Table 3 contains the results of comparisons of sO_2 and THb between each subgroup in malignant tissues only. In the case of ER and EGFR, statistical testing could not be performed due to the presence of only one ER^- and $EGFR^+$ sample, respectively. No statistical differences were observed in either the mean or the median sO_2 and THb in PR^+ versus PR^- tumor tissues. However, $HER2^+$ tumor tissues exhibited a statistically significant higher mean and median sO_2, and higher mean and median THb, than tissues not overexpressing the HER2/neu receptor.

No significant differences between malignant tissues taken from premenopausal and postmenopausal women could be determined in either sO_2 or THb, although the trend was for premenopausal tissues to have lower sO_2 and higher THb than postmenopausal tissues. Two of the sampled tumor tissues were from a single patient who had neoadjuvant chemotherapy; although there were not enough neoadjuvant samples to determine significant differences in sO_2 and THb from tissues not exposed to chemotherapy, the neoadjuvant samples exhibited markedly lower sO_2 and THb values than the mean and median for tissues from patients not undergoing neoadjuvant chemotherapy. Longitudinal studies, with prechemotherapy and postchemotherapy measurements, will be needed to determine whether chemotherapy has the general effect of reducing sO_2 and THb or whether the current results can be attributed to interpatient variability.

Discussion

Significant differences in tissue hemoglobin saturation exist between malignant and nonmalignant tissues in the breast, as has been seen in previous studies of the breast (18), oral cavity (19), and rectum/anus (20). It is well accepted that solid tumors are associated with decreased oxygen tension due to the increased oxygen demand of metabolically active cancer cells in combination with deficiencies in perfusion caused by a disordered and inefficient microvasculature created during the angiogenic process (21–26). In an important study by Vaupel and colleagues (26), polarographic oxygen electrodes were used to measure oxygen tension from ~50 sites in each of 16 normal tissues, 15 cancer tissues, and 5 fibrocystic tissues in the breast. In that report, the result of pooling all measurements for each tissue type together showed that breast cancer tissues exhibited a bimodal distribution of oxygen tension, with an overall lower median than normal tissues, whereas normal tissues exhibited a nearly Gaussian distribution of oxygen tension centered at higher values. Although our measurements arise from the vascular compartment, our results are consistent with those in that report, in that there is clearly tumor-to-tumor variability in oxygenation, giving rise to a nonuniform, multimodal tissue saturation distribution for malignant tissues. We observed a weighted distribution of sO_2 values for nonmalignant tissues, with the greatest number of tissues exhibiting 95% to 100% sO_2.

The presence of a significant number of malignant tissues with hemoglobin saturation values >80% prompted a deeper investigation into the characteristics of these tumors, particularly with regard to menopausal and hormone receptor status. Although the malignant samples were evenly balanced between premenopausal and postmenopausal status, no relationship was found between hemoglobin saturation or content, and menopausal status in these samples. No relationship between hemoglobin saturation and content, and ER or EGFR status could be calculated due to 19 of 20 malignant samples being ER^- and $EGFR^+$, respectively. Furthermore, no significant differences in hemoglobin saturation or content were observed between PR^- and PR^+ samples. However, we found that both hemoglobin saturation and total hemoglobin content were positively correlated with the extent of HER2/neu overexpression and that four of the five hypoxic tumors sampled in this study were negative for the HER2/neu receptor. HER2/neu overexpression is associated with a poor prognosis and has been implicated in tumors that are particularly aggressive and resistant to systemic therapies and local radiotherapy (27, 28). Breast cancers that overexpress HER2/neu are also associated with an increase in angiogenesis (29), primarily through up-regulation of HIF-1α and resultant vascular endothelial growth factor (VEGF) expression, via activation of the phosphoinositide-3-kinase/Akt pathway (28, 30). Our results show that hemoglobin saturation in tumors is positively correlated with the total hemoglobin concentration. This indicates that tumors that contain higher blood volume (and thus likely more vasculature due to angiogenesis) are better perfused and oxygenated than those with less dense vasculature. These findings are consistent with a model of increased angiogenesis and decreased tumor hypoxia promoted by HER2/neu overexpression. Thus, our results seem to indicate that (*a*) HER2/neu overexpression promotes angiogenesis in breast tumors and (*b*) this results in more highly perfused and well-oxygenated tumors.

Our results are supported by previous studies that noted the relationship between HER2/neu status, tumor angiogenesis, and tumor hypoxia (29, 31). In one study by Blackwell and colleagues (29), HER2/neu amplification was correlated with decreased tumor hypoxia and increased angiogenesis, as determined by FISH analysis of HER2/neu amplification, and immunohistochemical analysis of microvessel density (von Willebrand factor), the hypoxia marker CA IX, and VEGF, on previously biopsied tissues. In another study, Hohenberger and colleagues (31) analyzed pO_2 electrode measurements of breast tissues *in vivo* with respect to molecular growth determinants, including HER2/neu overexpression. The authors observed that tumors with higher HER2/neu overexpression (as determined by immunohistochemistry) had higher oxygenation, which agrees with our results.

The merits of the pO_2 electrode versus UV-visible optical spectroscopy are discussed below in the context of the type of tumor microenvironments that these technologies can probe and their methods of implementation. Several studies have investigated

Downloaded from http://aacrjournals.org/cancerres/article-pdf/69/7/2919/2622523/2919.pdf by guest on 14 September 2024

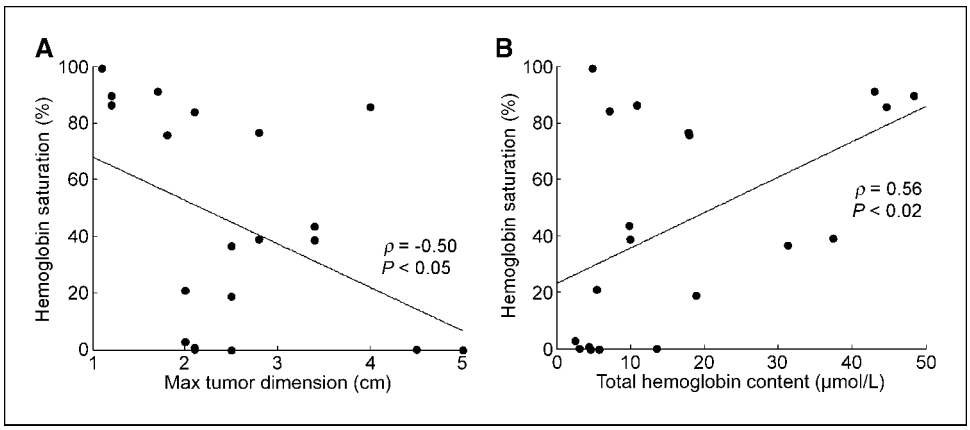

Figure 3. Tissue hemoglobin saturation as a function of tumor size (*A*) and total hemoglobin content (*B*) in malignant tissues only. *Inset,* Spearman's ρ and corresponding *P* values.

breast tumor oxygenation using the pO_2 electrode (26, 31–36). The advantages and disadvantages of pO_2 histography are well outlined in the recent review by Vaupel and colleagues (37). The primary attributes of the pO_2 electrode for measurement of tissue oxygenation are as follows: it can quantify actual tissue pO_2 and it can measure both perfusion-mediated (acute) as well as chronic hypoxia (at tissues far from the vasculature) because it does not rely on a measurement of vascular oxygenation alone. Although the pO_2 electrode can, in principle, isolate chronic from acute hypoxia, in practice, the electrode may be placed in the vasculature, interstitial space, or intracellularly for any given measurement (37). This uncertainty in electrode placement is usually overcome by taking tens to hundreds of measurements in any given tumor, with the resulting histograms likely reflective of both chronic and acute hypoxia. In contrast, the measurement reported with UV-visible optical spectroscopy is a volume-averaged measurement of the vascular oxygenation (including afferent and efferent vessels), and like other methods that measure vascular oxygenation, it is related to perfusion-mediated or acute hypoxia in tissues adjacent to the vasculature (38). Theoretical oxygen transport studies have indicated that although vascular O_2 supply is deterministic for tissue pO_2, vascular oxygenation is not always reflective of tissue oxygenation in all tumors due to intertumor variations in vascular geometry and arrangement (39–41). However, simultaneous measurement of total hemoglobin content (a surrogate for vascular extent) could aid in the interpretation of vascular oxygenation measurements, as it could identify tumors with sparse vasculature (where the difference between vascular and tissue pO_2 is expected to be greatest) from more well-perfused tumors (where vascular and tissue pO_2 are expected to be linearly related; ref. 40). In any case, it is not likely that a chronically hypoxic tumor would be characterized by well-oxygenated vasculature, meaning that measurement of vascular oxygenation can still identify a poorly oxygenated tumor, although there may not be a quantitative relationship

Table 3. Mean and median hemoglobin saturation and total hemoglobin content for subgroups of malignant tissues only

	n	Mean sO_2 (%)	Median sO_2 (%)	Mean THb (μmol/L)	Median THb (μmol/L)
$HER2^+$	6	76.9	87.7	29.6	30.9
$HER2^-$	14	30.6	28.7	11.7	8.5
		$P < 0.01$	$P < 0.02$	$P < 0.02$	$P < 0.05$
$EGFR^+$	1	99.1	99.1	4.8	4.8
$EGFR^-$	19	41.6	38.7	17.7	10.8
		—	—	—	—
ER^+	19	45.8	39.1	16.9	9.9
ER^-	1	18.9	18.9	18.9	18.9
		—	—	—	—
PR^+	15	40.8	36.6	18.6	10.8
PR^-	5	55.4	43.5	12.2	9.9
		n.s.	n.s.	n.s.	n.s.
Premenopausal	10	36.6	18.7	18.6	15.7
Postmenopausal	10	52.3	41.3	15.5	9.8
		n.s.	n.s.	n.s.	n.s.
Neoadjuvant	2	11.9	11.9	3.93	3.93
Primary surgery	18	48.1	41.3	18.5	12.1
		—	—	—	—

NOTE: *P* values are given to indicate significant differences in each subgroup.
Abbreviations: n.s., not significant; —, not calculated.

Downloaded from http://aacrjournals.org/cancerres/article-pdf/69/7/2919/2622523/2919.pdf by guest on 14 September 2024

between average vascular pO_2 and average tissue pO_2. Because vascular oxygenation cannot always be directly translated to clinical definitions of tumor hypoxia (which pertain to tissue pO_2 specifically), this suggests the need for further study to establish empirical relationships between tumor vascular oxygenation and radioresistance and chemoresistance, with the aim of identifying "sensitivity thresholds" for vascular oxygenation (as has been done for tissue oxygenation; ref. 1).

With respect to implementation, UV-visible optical spectroscopy offers several benefits over the pO_2 electrode in that it can continuously monitor changes in vascular oxygenation over short periods of time (because the probe does not consume oxygen) and it requires only a few measurements and thus less time to get an overall representation of acute hypoxia in a solid tumor because of its inherently larger sampling volume per placement (several cubic millimeters) compared with that of the pO_2 electrode (limited primarily to the surface of the electrode). Although this article specifically discussed vascular oxygenation measurements with light, UV-visible optical spectroscopy is sensitive to additional parameters, including tissue blood volume (via measurements of total hemoglobin absorbance), cell density, and/or proliferative status (via measurements of scattering; ref. 42), and can also be extended to measure cellular metabolism (via measurements of the fluorescence of cellular NADH and FAD), and can be extended into the near-IR regime for measurement of blood volume and saturation of superficial tumors from the tissue surface as shown by Chance and colleagues (43), Durduran and colleagues (44), Cerussi and colleagues (45), Tromberg and colleagues (46), Grosenick and colleagues (47), and Srinivasan and colleagues (48).

In conclusion, direct measurement of tumor vascular oxygenation via optical methods could be a viable method for clinical application. Due to its compatibility with commonly used biopsy needles, optical spectroscopy could be used at the time of core needle biopsy, providing an immediate measurement related to the extent of acute hypoxia in the tumor. This information could be used in conjunction with immunohistologic markers for chronic hypoxia to provide guidance to the oncologist about potential therapy options. In addition, measurement of acute hypoxia at diagnostic biopsy could aid in the interpretation of standard prognostic factors, for example, ER status, which is a useful biomarker for endocrine therapy but which has also been shown to be modulated by tumor hypoxia (49, 50). A previous study used quantitative UV-visible optical spectroscopy in the breast on a smaller number of patients (18). Although the sampling volume of that technique is roughly 2 orders of magnitude smaller than the one reported here, our results are consistent with those of that report and expand the available data on vascular oxygenation of the normal and diseased breast. Limitations of this study include (*a*) the ability to definitively measure the extent of chronic hypoxia in tissues distant from the vasculature and (*b*) the lack of available data on the clinical outcomes for patients enrolled in this study, precluding any interpretation of the prognostic or treatment-predictive value of these measurements. In future studies, we will perform longitudinal measurements in patients undergoing neoadjuvant systemic therapy, which could lead to the identification of relationships between vascular oxygenation, and response or resistance to therapy.

Disclosure of Potential Conflicts of Interest

No potential conflicts of interest were disclosed.

Acknowledgments

Received 8/29/08; revised 1/19/09; accepted 1/21/09; published OnlineFirst 3/17/09.

Grant support: NIH-National Cancer Institute (NCI) grant RO1 CA100559, Duke Comprehensive Cancer Center, and NIH-NCI grant F32 CA1240582 (J.Q. Brown).

The costs of publication of this article were defrayed in part by the payment of page charges. This article must therefore be hereby marked *advertisement* in accordance with 18 U.S.C. Section 1734 solely to indicate this fact.

We thank Drs. Mark Dewhirst and Karthik Vishwanath for helpful discussions and the staff of the Duke University Ambulatory Surgery Center for their invaluable assistance.

References

1. Hockel M, Vaupel P. Tumor hypoxia: definitions and current clinical, biologic, and molecular aspects. J Natl Cancer Inst 2001;93:266–76.
2. Hockel M, Schlenger K, Aral B, Mitze M, Schaffer U, Vaupel P. Association between tumor hypoxia and malignant progression in advanced cancer of the uterine cervix. Cancer Res 1996;56:4509–15.
3. Nordsmark M, Hoyer M, Keller J, Nielsen OS, Jensen OM, Overgaard J. The relationship between tumor oxygenation and cell proliferation in human soft tissue sarcomas. Int J Radiat Oncol Biol Phys 1996;35:701–8.
4. Brizel DM, Scully SP, Harrelson JM, et al. Tumor oxygenation predicts for the likelihood of distant metastases in human soft tissue sarcoma. Cancer Res 1996;56:941–3.
5. Trastour C, Benizri E, Ettore F, et al. HIF-1α and CA IX staining in invasive breast carcinomas: prognosis and treatment outcome. Int J Cancer 2007;120:1451–8.
6. Brown JM. Tumor hypoxia in cancer therapy. Methods Enzymol 2007;435:297–321.
7. Brown JM, Wilson WR. Exploiting tumour hypoxia in cancer treatment. Nat Rev Cancer 2004;4:437–47.
8. Evans SM, Koch CJ. Prognostic significance of tumor oxygenation in humans. Cancer Lett 2003;195:1–16.
9. Dewhirst MW, Klitzman B, Braun RD, Brizel DM, Haroon ZA, Secomb TW. Review of methods used to study oxygen transport at the microcirculatory level. Int J Cancer 2000;90:237–55.
10. Bender JE, Vishwanath K, Moore LK, et al. A robust Monte Carlo model for the extraction of biological absorption and scattering *in vivo*. IEEE Trans Biomed Eng. In press 2009.
11. Palmer GM, Ramanujam N. Monte Carlo-based inverse model for calculating tissue optical properties. Part I. Theory and validation on synthetic phantoms. Appl Opt 2006;45:1062–71.
12. Vishwanath K, Yuan H, Moore L, Bender J, Dewhirst M, Ramanujam N. Longitudinal monitoring of 4T1-tumor physiology *in vivo* with doxorubicin treatment via diffuse optical spectroscopy. Biomedical optics/digital holography and three-dimensional imaging/laser applications to chemical, security and environmental analysis. St. Petersburg (FL): The Optical Society of America; 2008.
13. Skala MC, Palmer GM, Vrotsos KM, Gendron-Fitzpatrick A, Ramanujam N. Comparison of a physical model and principal component analysis for the diagnosis of epithelial neoplasias *in vivo* using diffuse reflectance spectroscopy. Opt Express 2007;15:7863–75.
14. Palmer GM, Ramanujam N. Monte-Carlo-based model for the extraction of intrinsic fluorescence from turbid media. J Biomed Opt 2008;13:024017.
15. Zhu CF, Palmer GM, Breslin TM, Harter J, Ramanujam N. Diagnosis of breast cancer using diffuse reflectance spectroscopy: comparison of a Monte Carlo versus partial least squares analysis based feature extraction technique. Lasers Surg Med 2006;38:714–24.
16. Palmer GM, Zhu CF, Breslin TM, Xu FS, Gilchrist KW, Ramanujam N. Monte Carlo-based inverse model for calculating tissue optical properties. Part II. Application to breast cancer diagnosis. Appl Opt 2006;45:1072–8.
17. Manz R, Otte J, Thews G, Vaupel P. Relationship between size and oxygenation status of malignant tumors. Adv Exp Med Biol 1983;159:391–8.
18. van Veen RL, Amelink A, Menke-Pluymers M, van der Pol C, Sterenborg HJ. Optical biopsy of breast tissue using differential path-length spectroscopy. Phys Med Biol 2005;50:2573–81.
19. Mueller-Klieser W, Vaupel P, Manz R, Schmidseder R. Intracapillary oxyhemoglobin saturation of malignant tumors in humans. Int J Radiat Oncol Biol Phys 1981;7:1397–404.
20. Wendling P, Manz R, Thews G, Vaupel P. Heterogeneous oxygenation of rectal carcinomas in humans: a critical parameter for preoperative irradiation? Adv Exp Med Biol 1984;180:293–300.
21. Vaupel P. The role of hypoxia-induced factors in tumor progression. Oncologist 2004;9 Suppl 5:10–7.
22. Vaupel P, Harrison L. Tumor hypoxia: causative factors, compensatory mechanisms, and cellular response. Oncologist 2004;9 Suppl 5:4–9.
23. Vaupel P, Hockel M. Blood supply, oxygenation status and metabolic micromilieu of breast cancers: characterization and therapeutic relevance. Int J Oncol 2000;17:869–79.
24. Vaupel P, Kelleher DK, Hockel M. Oxygen status of malignant tumors: pathogenesis of hypoxia and significance for tumor therapy. Semin Oncol 2001;28:29–35.
25. Vaupel P, Mayer A, Hockel M. Tumor hypoxia and malignant progression. Methods Enzymol 2004;381:335–54.
26. Vaupel P, Schlenger K, Knoop C, Hockel M. Oxygenation of human tumors: evaluation of tissue oxygen

Downloaded from http://aacrjournals.org/cancerres/article-pdf/69/7/2919/2622523/2919.pdf by guest on 14 September 2024

distribution in breast cancers by computerized O_2 tension measurements. Cancer Res 1991;51:3316–22.
27. Alaoui-Jamali MA, Paterson J, Al Moustafa AE, Yen L. The role of ErbB-2 tyrosine kinase receptor in cellular intrinsic chemoresistance: mechanisms and implications. Biochem Cell Biol 1997;75:315–25.
28. Zhou BP, Li Y, Hung MC. HER-2/Neu signaling and therapeutic approaches in breast cancer. Breast Dis 2002;15:13–24.
29. Blackwell KL, Dewhirst MW, Liotcheva V, et al. HER-2 gene amplification correlates with higher levels of angiogenesis and lower levels of hypoxia in primary breast tumors. Clin Cancer Res 2004;10:4083–8.
30. Laughner E, Taghavi P, Chiles K, Mahon PC, Semenza GL. HER2 (neu) signaling increases the rate of hypoxia-inducible factor 1α (HIF-1α) synthesis: novel mechanism for HIF-1-mediated vascular endothelial growth factor expression. Mol Cell Biol 2001;21:3995–4004.
31. Hohenberger P, Felgner C, Haensch W, Schlag PM. Tumor oxygenation correlates with molecular growth determinants in breast cancer. Breast Cancer Res Treat 1998;48:97–106.
32. Falk SJ, Ward R, Bleehen NM. The influence of carbogen breathing on tumour tissue oxygenation in man evaluated by computerised pO_2 histography. Br J Cancer 1992;66:919–24.
33. Jones EL, Prosnitz LR, Dewhirst MW, et al. Thermochemoradiotherapy improves oxygenation in locally advanced breast cancer. Clin Cancer Res 2004;10:4287–93.
34. Runkel S, Wischnik A, Teubner J, Kaven E, Gaa J, Melchert F. Oxygenation of mammary tumors as evaluated by ultrasound-guided computerized-pO_2-histography. Adv Exp Med Biol 1994;345:451–8.
35. Vaupel P, Mayer A, Briest S, Hockel M. Oxygenation gain factor: a novel parameter characterizing the association between hemoglobin level and the oxygenation status of breast cancers. Cancer Res 2003;63:7634–7.
36. Vujaskovic Z, Rosen EL, Blackwell KL, et al. Ultrasound guided pO_2 measurement of breast cancer reoxygenation after neoadjuvant chemotherapy and hyperthermia treatment. Int J Hyperthermia 2003;19:498–506.
37. Vaupel P, Hockel M, Mayer A. Detection and characterization of tumor hypoxia using pO_2 histography. Antioxid Redox Signal 2007;9:1221–35.
38. Padhani AR, Krohn KA, Lewis JS, Alber M. Imaging oxygenation of human tumours. Eur Radiol 2007;17:861–72.
39. Dasu A, Toma-Dasu I. The relationship between vascular oxygen distribution and tissue oxygenation. Adv Exp Med Biol 2009;645:255–60.
40. Dasu A, Toma-Dasu L. Vascular oxygen content and the tissue oxygenation—a theoretical analysis. Med Phys 2008;35:539–45.
41. Thews G, Vaupel P. O_2 supply conditions in tumor tissue *in vivo*. Adv Exp Med Biol 1976;75:537–46.
42. Mourant JR, Canpolat M, Brocker C, et al. Light scattering from cells: the contribution of the nucleus and the effects of proliferative status. J Biomed Opt 2000;5:131–7.
43. Chance B, Nioka S, Zhang J, et al. Breast cancer detection based on incremental biochemical and physiological properties of breast cancers: a six-year, two-site study. Acad Radiol 2005;12:925–33.
44. Durduran T, Choe R, Culver JP, et al. Bulk optical properties of healthy female breast tissue. Phys Med Biol 2002;47:2847–61.
45. Cerussi A, Hsiang D, Shah N, et al. Predicting response to breast cancer neoadjuvant chemotherapy using diffuse optical spectroscopy. Proc Natl Acad Sci U S A 2007;104:4014–9.
46. Tromberg BJ, Shah N, Lanning R, et al. Non-invasive *in vivo* characterization of breast tumors using photon migration spectroscopy. Neoplasia 2000;2:26–40.
47. Grosenick D, Wabnitz H, Moesta KT, et al. Concentration and oxygen saturation of haemoglobin of 50 breast tumours determined by time-domain optical mammography. Phys Med Biol 2004;49:1165–81.
48. Srinivasan S, Pogue BW, Jiang SD, et al. Interpreting hemoglobin and water concentration, oxygen saturation, and scattering measured *in vivo* by near-infrared breast tomography. Proc Natl Acad Sci U S A 2003;100:12349–54.
49. Kronblad A, Hedenfalk I, Nilsson E, Pahlman S, Landberg G. ERK1/2 inhibition increases antiestrogen treatment efficacy by interfering with hypoxia-induced downregulation of ERα: a combination therapy potentially targeting hypoxic and dormant tumor cells. Oncogene 2005;24:6835–41.
50. Cooper C, Liu GY, Niu YL, Santos S, Murphy LC, Watson PH. Intermittent hypoxia induces proteasome-dependent down-regulation of estrogen receptor α in human breast carcinoma. Clin Cancer Res 2004;10:8720–7.

Downloaded from http://aacrjournals.org/cancerres/article-pdf/69/7/2919/2622523/2919.pdf by guest on 14 September 2024